Implementation and Validation of a CubeSat Laser Transmitter*

R.W. Kingsbury[a,c], D.O. Caplan[b], K.L. Cahoy[c]

[a]Planet Labs, 346 9th Street, San Francisco, CA 94103;
[b]MIT Lincoln Laboratory, 244 Wood Street, Lexington, MA 02420;
[c]Massachusetts Institute of Technology, 77 Massachusetts Ave, Cambridge, MA 02139

ABSTRACT

The paper presents implementation and validation results for a CubeSat-scale laser transmitter. The master oscillator power amplifier (MOPA) design produces a 1550 nm, 200 mW average power optical signal through the use of a directly modulated laser diode and a commercial fiber amplifier. The prototype design produces high-fidelity M-ary pulse position modulated (PPM) waveforms (M=8 to 128), targeting data rates > 10 Mbit/s while meeting a constraining 8 W power allocation. We also present the implementation of an avalanche photodiode (APD) receiver with measured transmitter-to-receiver performance within 3 dB of theory. Via loopback, the compact receiver design can provide built-in self-test and calibration capabilities, and supports incremental on-orbit testing of the design.

Keywords: free-space optical communications, CubeSat, small satellites, optical transmitters, lasercom

1. INTRODUCTION

In this paper, we present the implementation and validation of a MOPA-based laser transmitter suitable for use in severely size, weight and power (SWaP) constrained CubeSats. A commercial off the shelf (COTS) based approach was taken to achieve a design that is compatible with CubeSat cost and lead time constraints. The transmitter produces a high-fidelity, 200 mW average power optical output signal at 1550 nm with less than 8 W electrical input power. These results build upon previously reported architectural studies for both the top-level CubeSat lasercom system as well as the transmitter subsystem.[1,2] This lasercom system design has been optimized for providing direct downlink (space to ground) from low-earth orbit (LEO) CubeSats to a low-cost ground aperture (30 cm) using an APD-based receiver. The system is designed to provide channel rates between 10.9 Mbps (128-PPM) and 75 Mbps (8-PPM) at bit error rates less than 10^{-4}.

The transmitter design consists of an FPGA-driven directly modulated laser (DML) that generates M-ary pulse position modulation (PPM) waveforms at a slot rate of 200 MHz. The modulation-induced chirp of the DML output is used in conjunction with a narrow fiber Bragg grating filter, which performs FM-to-AM conversion[3–6] that improves the modulation extinction ratio (ER) in this transmitter design to greater than 40 dB. The low duty cycle (8-PPM through 128-PPM) signal is subsequently amplified by a COTS Erbium-doped Fiber Amplifier (EDFA) operating in saturation so that the peak transmit power approaches 25 W in the lowest rate mode (128-PPM, 10.9 Mbps).

The transmitter also incorporates a variety of built-in self-test (BIST) features that facilitate testing and calibration both in the lab and while operating in orbit. Implementation of the BIST functions have minimal impact on size, weight, and power since they can be straightforwardly implemented with the addition of a coupler, photodiode, and comparator, and can leverage spare logic resources available in the FPGA. This enables in-situ measurement of important transmitter performance metrics such as peak power and ER. BIST can also operate as

* The Lincoln Laboratory portion of this work is sponsored by the Assistant Secretary of Defense for Research & Engineering under Air Force Contract #FA8721–05–C–0002. Opinions, interpretations, conclusions and recommendations are those of the author and are not necessarily endorsed by the United States Government.

Send correspondence to R.W. Kingsbury (ryan.kingsbury (at) gmail.com)

Free-Space Laser Communication and Atmospheric Propagation XXVIII, edited by Hamid Hemmati, Don M. Boroson, Proc. of SPIE Vol. 9739, 973905 · © 2016 SPIE
CCC code: 0277-786X/16/$18 · doi: 10.1117/12.2217990

a loopback receiver to validate sensitivity of the communications detector. Using this capability, net transmitter-to-receiver communication performance was measured within 3 dB from theoretical predictions. Theoretical predictions for system performance were obtained using Q-factor analysis that were principally limited by APD thermal noise. A vendor-provided noise equivalent power (NEP) specification was used in this analysis.

2. TRANSMITTER DESIGN VALIDATION

In this section, we present experimental results which confirm the average-power-limited behavior of the transmitter. The peak output power of the transmitter directly impacts the system link budget for multiple reasons. First, receiver performance is limited by the thermal noise floor of the avalanche photodiode (APD), so the use of high-peak-power low-duty-cycle waveforms provides a means of improving the detected signal-to-noise ratio (SNR) given an average-power-limited source.[7,8] In addition, since the number of bits per symbol grows as the PPM symbol size M is increased (and corresponding duty cycle is decreased), this also improves the receiver sensitivity as measured in photons/bit.[9] As a result, changes in waveform duty cycle M are are selected as the primary means through which the system adapts to changing link conditions. In order to efficiently deliver the EDFA's average-power-limited output to the PPM waveform and avoid power-robbing transmitter penalties,[9,10] the transmitter modulation ER must be much larger than M, i.e. ER $>$ M + 15 dB, and this becomes more challenging for large M. Therefore, power-sensitive applications with duty cycles as low as $M = 1/128$ (i.e., 128-PPM) that require ER $>$ 36 dB, it is important to be able measure and optimize the peak signal output power to confirm adequate transmitter ER and EDFA gain, and ensure efficient transmitter operation.[11,12] Previously, we reported ER measurements of the source seed laser >40 dB that were collected using a swept duty cycle measurement approach.[2]

Figure 1 shows the achieved peak output power from the EDFA at duty cycles between 8-PPM and 128-PPM. This data was collected with a calibrated linear photodiode and a high-speed oscilloscope. As constructed, the prototype is able to deliver peak power levels within 0.18 dB of predicted performance at the lowest duty cycle mode (128-PPM). This small amount of implementation loss is likely the result of slightly under-driving the EDFA input signal so that it is no longer operating in the deeply saturated regime and extracting maximum average output power.

3. LOOPBACK RECEIVER & END-TO-END LINK VALIDATION

Testing end-to-end communications link performance was a high priority during the validation effort. The achievable data rate of the system operating over the LEO to ground link[1,2] is limited by the noise parameters of the communications detector, a COTS APD module[†]. Therefore, validating the vendor noise specification of this device was a crucial step towards building confidence in the link budget.

Instead of implementing a stand-alone PPM receiver, we implemented a low-complexity "loopback" receiver (Figure 2), which can be used to provide real-time feedback on transmitter performance.[12–14] This receiver consists of a comparator-based analog front-end that converts the input analog electrical signal into digital for processing by the FPGA. A digital to analog converter (DAC) is used to generate a threshold voltage that can be adjusted to optimize the error rate.[15]

Inside the FPGA, the received digital signal is compared to a delayed copy of the transmit signal. Differences between the two bit streams are identified with an exclusive-OR (XOR) gate and subsequently counted. The FPGA also keeps count of the total number of cycles that have elapsed which allows calculation of a slot error rate (SLER). Given knowledge of the PPM order M, it is possible to map SLER into a symbol error rate and, subsequently, bit error rate (BER).The loopback receiver implementation is further simplified since it can leverage the same reference clock as the transmitter. so it is not necessary to implement clock and data recovery (CDR) functionality.

Most communication systems are validated in an end-to-end fashion through the measurement of BER curves, or data that shows how BER degrades as the receiver's input power is decreased. The transmitter optical output is attenuated to levels comparable to those predicted by the system link budget suitable so that receiver

[†]The APD module includes a trans-impedance amplifier and a single-stage thermometric cooler.

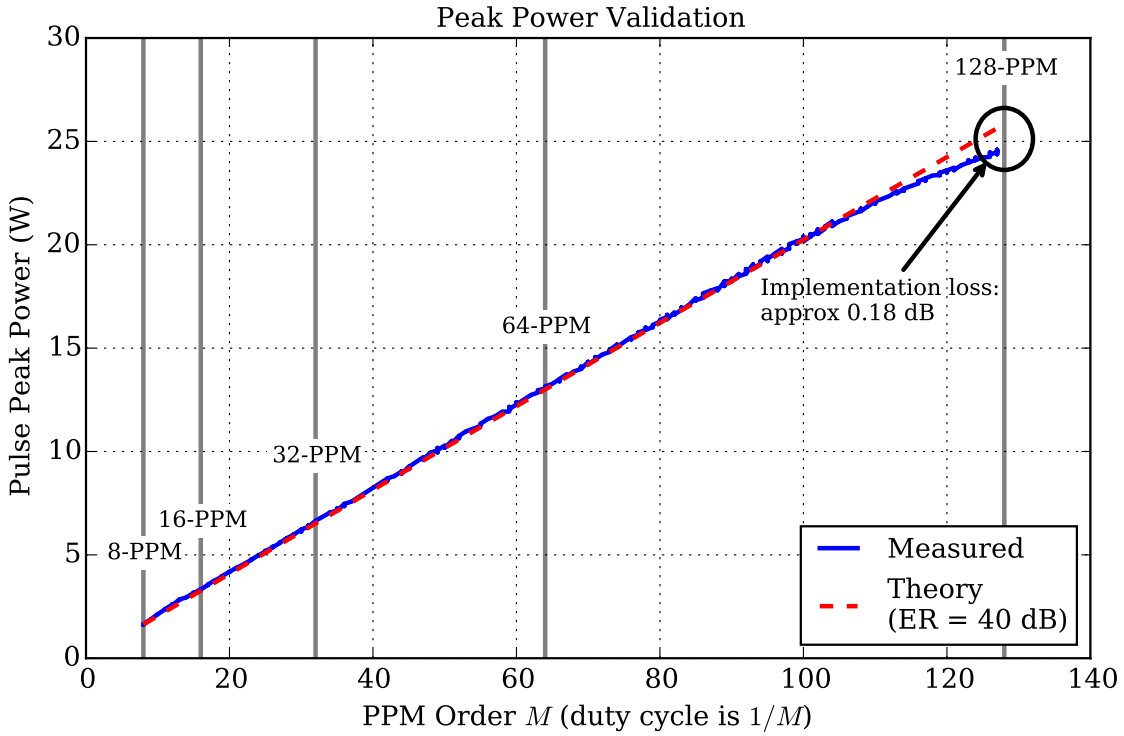

Figure 1. A linear photodiode was used to measure the peak output power of the EDFA at various duty cycles. The design exhibits average-power-limited behavior and produces peak output power levels to within 0.18 dB of predicted performance. The theory curve represents an ideal transmitter incorporating a finite ER = 40 dB seed laser.

performance can be measured and validated. The attenuation simulates the aperture gain terms, path loss, and other loss terms contained in the system link budget. Attenuation is generally swept from the error-free regime (BER ≈ 0) to the point where the error rate has reached the maximum possible value (BER = 0.5).

The fully automated BER curve measurement process greatly improved experimental repeatability and facilitated the acquisition and processing of many trials. An operating point for the transmitter is defined by the tuple (M, L_{atten}). At each operating point two additional degrees of freedom exist in the receiver: the value of the delay block t_{delay} and the value of the threshold voltage, V_{DAC}. The value of t_{delay} matches the delay of the signal as it propagates through the seed laser, extinction filter, EDFA, attenuators, and detector circuit. In practice, this was measured once with an oscilloscope and then hard-coded in the automation script. The optimal value of V_{DAC} (i.e., the value that minimizes BER) depends on the signal levels present at the comparator input. To find this value, the test automation script exhaustively tests all possible values and reports the best BER found during the search. This process is repeated at every (M, L_{atten}) operating point. The BER automation script also collects power meter measurements to precisely document the input power to the detector.

Once collected, the data is post-processed to incorporate calibration parameters from the test apparatus (e.g., coupler ratios). The receiver power figure is also normalized into photons-per-bit for comparative purposes. The measured data shows that the receiver is approximately 2.4 dB to 3.0 dB less sensitive than predicted depending on the mode. Lower rate modes, such as 128-PPM, are closer to the predicted sensitivity than the high rate modes (e.g., 8-PPM). Both measured and predicted BER curves are given in Figure 3. Figure 4 shows BER curves versus APD input power.

The rate-dependent sensitivity variations of the prototype system have been the subject of much scrutiny. In the predicted sensitivity analysis,[2] the detector APD and its noise parameters set the overall sensitivity of the system. In the current laboratory prototype, we believe electrical noise sources after the APD/TIA module,

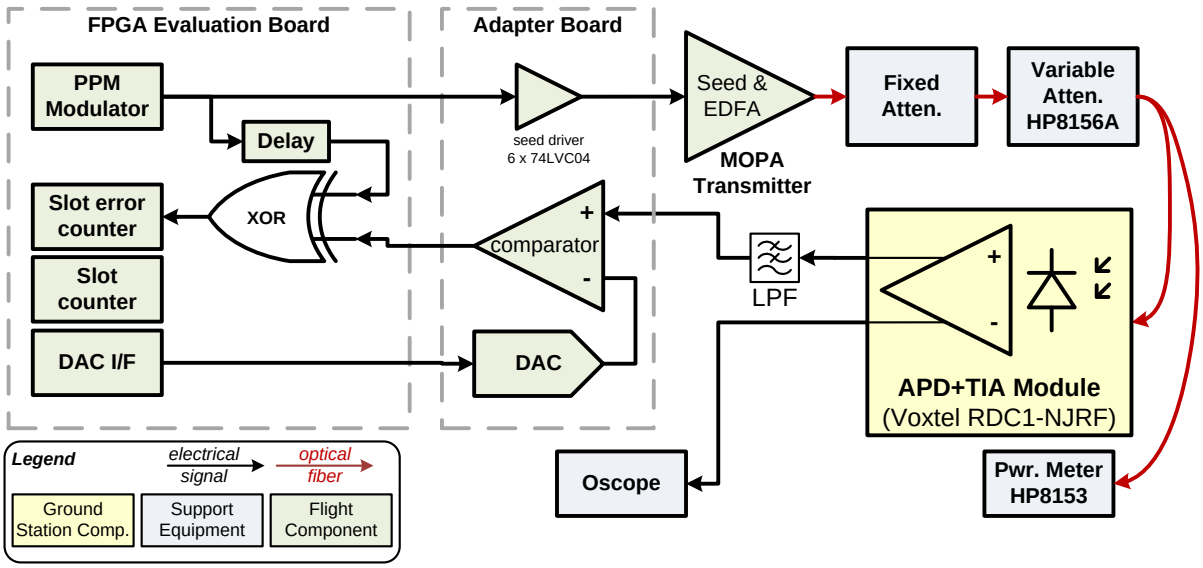

Figure 2. The loopback receiver compares the received digital signal to a delayed version of the transmit signal in order to infer slot-error-rate. A DAC and a comparator form a 1-bit ADC that is used to convert the input analog waveform into a digital signal.

especially on the "adapter board" which hosts the comparator decision circuit (see Figure 2) may be responsible. The seed laser modulation traces lie in close proximity to the decision circuit so crosstalk is likely an issue. Despite the extraneous noise contribution, the experimental demonstration of performance within 3 dB of that predicted is a valuable result from the prototype system. While additional refinement of both the hardware and link budget analysis will be pursued in the future, these measurements provide a useful measurement baseline.

4. BUILT-IN SELF-TEST

The loopback receiver has utility beyond laboratory or ground-based testing,[12–14,16] since a variant of this receiver can be integrated into the flight design to provide a built-in self-test (BIST) functionality. With this configuration, BIST provides important diagnostic information about the health of the optical transmitter. And in the event of failure of the pointing, acquisition and tracking (PAT) subsystem, this receiver can be used to establish partial mission success through on-orbit validation of the transmitter.

For a flight variant of the loopback receiver, it is not necessary to use a high-sensitivity cooled APD/TIA module. Instead, low-power fiber-coupled photodiode(s) can be used to monitor the transmit signal at various points in the transmitter chain. Monitoring the signal at strategic points in the transmitter chain can give insight into the operating performance of the transmitter (Figure 5).

Given a transmitted signal $x(t)$, we assume that the BIST system has monitoring capability at three points along the transmit chain:

- $y_A(t)$ is proportional to the EDFA output which includes peak power gains imparted by the average-power-limited amplification process
- $y_B(t)$ is proportional to the EDFA input, nominally a high ER signal consisting of "mark" symbols
- $y_C(t)$ is the seed signal rejected by the FBG filter, also nominally a high ER signal but consisting purely of "space" symbols

Each of the monitor points is connected to a comparator with a variable threshold as described in Section 3. The FPGA provides the ability to measure slot error rate (SLER) as well as the occurrence rate of high ("mark") and low ("space") slots.

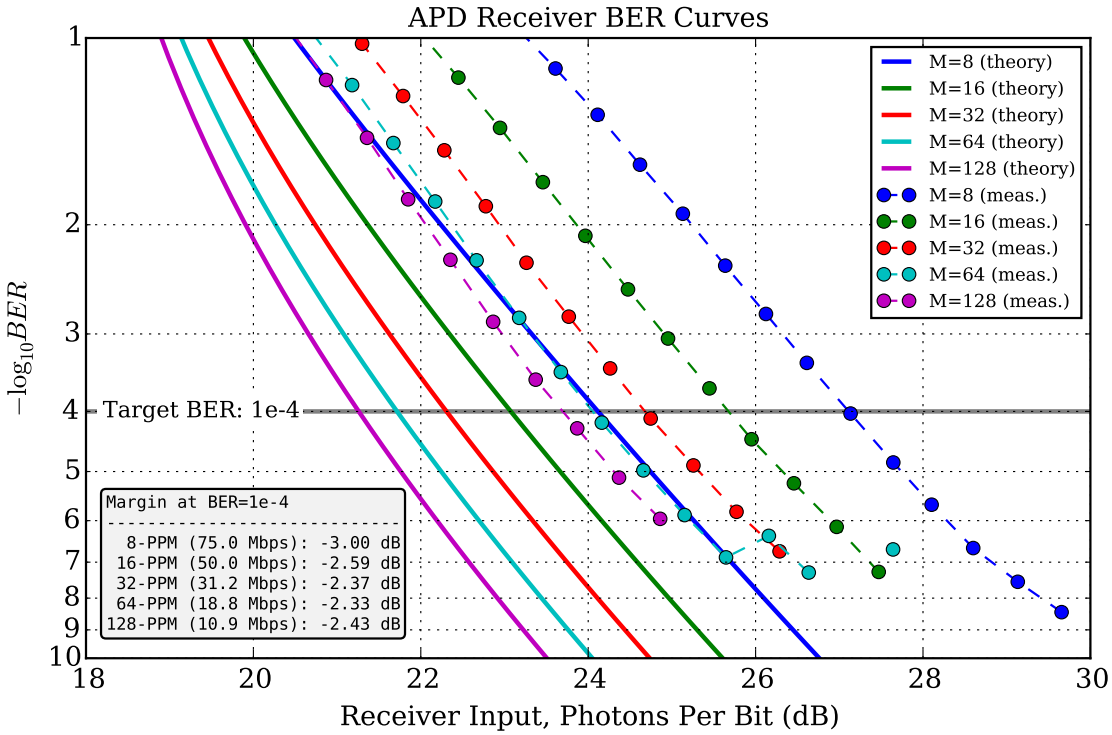

Figure 3. Bit error rate (BER) curves for the end-to-end communication link including the prototype transmitter and fiber-coupled variant of the ground station APD/TIA receiver module. The design is 2.4 dB to 3.0 dB from predicted sensitivity. The source of this descrepancy is currently under investigation, but electrical crosstalk between the seed laser driver and the comparator decision circuit is suspected.

Monitor signal $y_A(t)$ can be use to estimate peak power without the use of bulky laboratory-grade equipment. The decision threshold voltage is adjusted to find the peak of the optical waveform (a similar design is presented in reference[15]) using *a priori* knowledge of the transmit waveform duty cycle. Additional details about the measurement approach are presented in a related work.[2]

Experimental results which validate this measurement technique are shown in Figure 6. The transmitter peak output power was varied by changing the modulation order M. The peak power estimation feature of the BIST receiver was used to collect peak power estimates, while a high-speed oscilloscope measured a truth value. The measurement technique has strong correlation ($R^2 = 0.9993$) with the truth value and is usable is a transmitter output figure of merit.

The two additional BIST signals, $y_B(t)$ and $y_C(t)$, can be used to assist with frequency alignment of the seed laser with the passband of the FBG filter. Even though an athermal FBG filter has been used in this design, the center frequency of this filter still changes with temperature (approximately 4 GHz over the 0 °C to 40 °C operating range), more than enough to impact transmitter performance. Alignment within roughly 2 GHz (related to the filter bandwidth) is necessary to ensure that the EDFA drive waveform has sufficient ER.[1]

The $y_B(t)$ and $y_C(t)$ signals, when combined with knowledge of the waveform duty cycle, can be used to estimate optical energy present in both the passband and the stopband of the FBG filter. These metrics can be used to determine if the seed laser is tuned "too high" or "too low" relative to the FBG filter. An area of future work is to use these signals to close a control loop around the seed laser wavelength tuning (by way of temperature and DC bias settings) [‡].

[‡]Absolute frequency stability is not essential for this application as the ground station has a wide (>2 nm) input filter.

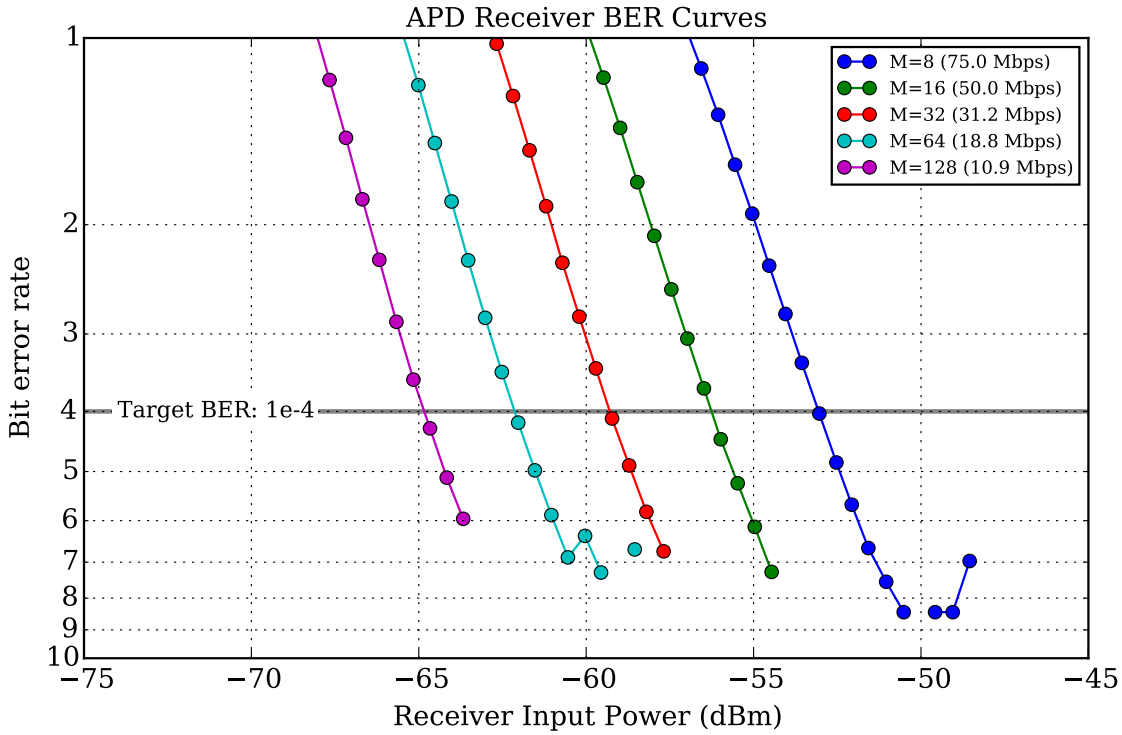

Figure 4. Bit error rate (BER) curves versus detector input power for the end-to-end communication link including the prototype transmitter and fiber-coupled variant of the ground station APD/TIA receiver module.

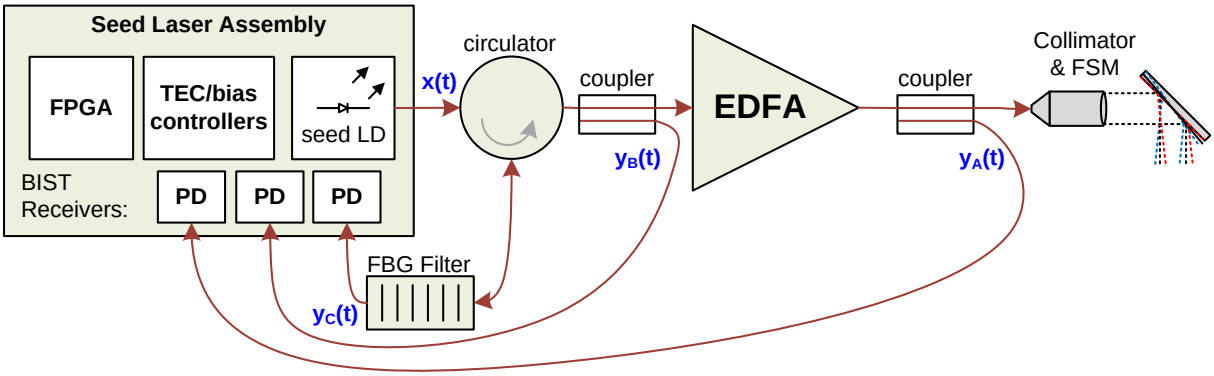

Figure 5. BIST functionality expands upon the loopback receiver design by monitoring the transmitter optical chain at various points. Each of these signals can be converted to the digital domain (configurable threshold) and compared to delayed copies of the transmit signal.

5. CONCLUSIONS

This paper has presented the implementation and validation measurements of a low-SWaP MOPA-based laser transmitter prototype. This transmitter produces 1550 nm, 200 mW average power optical output with high ER (>40 dB), which enables the use of low duty cycle waveforms such as 128-PPM. Peak output power measurements confirm that the design is providing average-power-limited behavior across the 8-PPM (10.9 Mbps) to 128-PPM (75 Mbps) operating range. A novel loopback receiver was used to measure the end-to-end link performance of the prototype transmitter and the APD selected for the system. These measurements show end-to-end performance

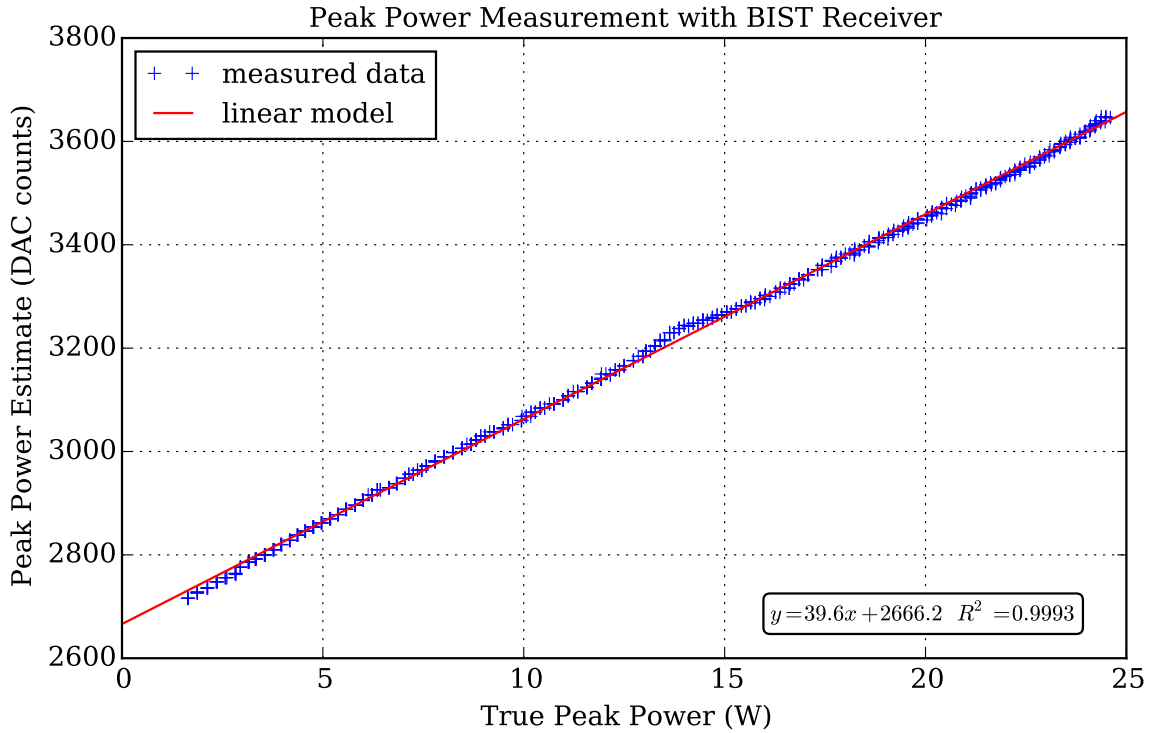

Figure 6. Peak power estimation measurement results using the BIST receiver as compared to true peak power measured with a highly linear photodiode and oscilloscope. A linear relationship ($R^2 = 0.9993$) exists between the truth data and the measurement.

that is within 3 dB of predictions. Finally, we described built-in self-test (BIST) functionality which can be incorporated into the transmitter design with minimal additional hardware. The BIST functionality provides a means for optimization of ER and peak output power of the transmitter.

REFERENCES

[1] Kingsbury, R. W., Caplan, D. O., and Cahoy, K. L., "Compact optical transmitters for cubesat free-space optical communications," in [*Proc. SPIE 9354*], *Proc. SPIE* **9354**, 93540S–93540S–7 (2015).

[2] Kingsbury, R. W., *Optical Communications for Small Satellites*, PhD thesis, Massachusetts Institute of Technology (2015).

[3] Vodhanel, R. S., Elrefaie, A. F., Iqbal, M., Wagner, R. E., Gimlett, J., and Tsuji, S., "Performance of directly modulated dfb lasers in 10-Gb/s ASK, FSK, and DPSK lightwave systems," *Lightwave Technology, Journal of* **8**(9), 1379–1386 (1990).

[4] Lee, C.-H., Lee, S.-S., Kim, H. K., and Han, J.-H., "Transmission of directly modulated 2.5-Gb/s signals over 250-km of nondispersion-shifted fiber by using a spectral filtering method," *Photonics Technology Letters, IEEE* **8**(12), 1725–1727 (1996).

[5] Mahgrefteh, D., Cho, P., Goldhar, J., and Mandelberg, H., "Penalty-free propagation over 600 km of non-dispersion-shifted fiber at 2.5-Gb/s using a directly laser modulated transmitter," in [*Lasers and Electro-Optics, 1999. CLEO'99. Summaries of Papers Presented at the Conference on*], 182, IEEE (1999).

[6] Caplan, D. O. and Carney, J., "Power-efficient noise-insensitive optical modulation for high-sensitivity laser communications," in [*CLEO: Science and Innovations*], SM4J–6, Optical Society of America (2014).

[7] Boivin, L., Nuss, M. C., Shah, J., B., M. D. A., and Haus, H. A., "Receiver sensitivity improvement by impulsive coding," *Photonics Technology Letters, IEEE* **9**, 684–686 (1997).

[8] Caplan, D. O., Stevens, M. L., Boroson, D. M., and Kaufmann, J. E., "A multi-rate optical communications architecture with high sensitivity," in [*Lasers and Electro-Optics Society, 1999. LEOS 1999. The 12th Annual Meeting of the IEEE*], (1999).

[9] Caplan, D. O., "Laser communication transmitter and receiver design," *Journal of Optical and Fiber Communications Reports* **4**(4-5), 225–362 (2007).

[10] Caplan, D. O., Robinson, B. S., Murphy, R. J., and Stevens, M. L., "Demonstration of 2.5 Gslot/s optically-preamplified M-PPM with 4 photons/bit receiver sensitivity," in [*Optical Fiber Communication Conference (OFC)*], PDP32, Optical Society of America (2005).

[11] Caplan, D., "A technique for measuring and optimizing modulator extinction ratio," in [*Lasers and Electro-Optics, 2000.(CLEO 2000). Conference on*], 335–336, IEEE (2000).

[12] Caplan, D., Carney, J., Lafon, R., and Stevens, M., "Design of a 40 watt 1.55 μm uplink transmitter for lunar laser communications," in [*SPIE LASE*], 82460M–82460M, International Society for Optics and Photonics (2012).

[13] Caplan, D., Carney, J., Fitzgerald, J., Gaschits, I., Kaminsky, R., Lund, G., Hamilton, S., Magliocco, R., Murphy, R., Rao, H., et al., "Multi-rate DPSK optical transceivers for free-space applications," in [*SPIE LASE*], 89710K–89710K, International Society for Optics and Photonics (2014).

[14] Spellmeyer, N., Browne, C., Caplan, D., Carney, J., Chavez, M., Fletcher, A., Fitzgerald, J., Kaminsky, R., Lund, G., Hamilton, S., et al., "A multi-rate DPSK modem for free-space laser communications," in [*SPIE LASE*], 89710J–89710J, International Society for Optics and Photonics (2014).

[15] Spellmeyer, N. W., Bernstein, S. L., Boroson, D. M., Caplan, D. O., Fletcher, A. S., Hamilton, S. A., Murphy, R. J., Norvig, M., Rao, H. G., Robinson, B. S., et al., "Demonstration of multi-rate thresholded preamplified 16-ary pulse-position-modulation," in [*Optical Fiber Communication Conference*], OThT5, Optical Society of America (2010).

[16] Wang, J. P., Browne, C., Burton, C., Caplan, D., Carney, J., Chavez, M., Fitzgerald, J., Gaschits, I., Geisler, D., Hamilton, S., et al., "Performance and qualification of a multi-rate DPSK modem," in [*SPIE LASE*], 89710Z–89710Z, International Society for Optics and Photonics (2014).